

## Numerical studies of the formation and decay of electron-hole plasma clusters in highly excited direct-gap semiconductors

H. Haug\* and Farid F. Abraham

IBM Research Laboratory, San Jose, California 95193

(Received 14 July 1980)

The master equation for the cluster-size distribution function is solved numerically for the example of GaAs excited by various laser pulses. The results show that the steady-state distribution would be obtained only with excitation pulses which last around 100 ns. The formation and decay of the small clusters which are created under typical nano- and picosecond-pulse excitations are calculated, as well as the time dependence of various quantities which are relevant for experimental observations.

### I. THE MASTER EQUATION FOR THE ELECTRON-HOLE NUCLEATION KINETICS

In photoexcited semiconductors one observes at low temperatures a nonequilibrium phase transition from a low-density exciton gas phase to a high-density liquid plasma phase. In semiconductors with an indirect gap and correspondingly long optical lifetimes, such as Ge and Si, this phase transition has been investigated experimentally in great detail.<sup>1</sup> Within the coexistence region relatively large electron-hole ( $e-h$ ) clusters are formed. The kinetics of the  $e-h$  droplet formation is well understood in terms of the master equation for the concentrations of clusters of various sizes.<sup>2-5</sup> This theoretical approach is a natural extension of the classical nucleation theory<sup>6</sup> to a nonequilibrium system. Because the average number of  $e-h$  pairs per cluster is large (for Ge typically  $\langle n \rangle \approx 10^6$ ), the master equation is usually approximated by considering  $n$  as a continuous variable. With this approximation the master equation reduces to the Fokker-Planck equation for which various approximation schemes exist.<sup>2,4,5,7</sup>

In direct-gap semiconductors, such as GaAs and CdS, the existence of an  $e-h$  plasma liquid at low temperatures has also been established,<sup>8</sup> but not much is known about the details of the phase transition. Intuitively, one would expect that due to the short lifetime (typically 1 ns), only small  $e-h$  clusters can be formed and sustained. Under these conditions one has to treat the master equation of the nucleation kinetics directly in its discrete version, i.e., one has to treat the number  $n$  of  $e-h$  pairs per cluster as an integer. The growth and decay of a cluster is determined by the rates at which excitons ( $x$ ) are collected and evaporated by the cluster and by the recombination rate of  $e-h$  pairs within the cluster. The probability  $f_n(t)$  to find at a given time  $t$  a cluster with  $n$   $e-h$  pairs per unit volume is given by the fol-

lowing equation:

$$\frac{\partial f_n}{\partial t} = j_{n-1} - j_n \quad \text{for } n > 1, \quad (1)$$

where  $j_n$  is the net probability current between the clusters with  $n$  and  $n+1$   $e-h$  pairs,

$$j_n = g_n f_n - l_{n+1} f_{n+1}, \quad (2)$$

where

$$l_n = e_n + n/\tau_n.$$

Here,  $g_n$  is the gain rate which describes the rate at which excitons are collected at the surface of a cluster with  $n$   $e-h$  pairs and is approximated by

$$g_n = 4\pi R_n^2 v_x f_1,$$

where

$$v_x = \frac{kT}{2\pi m_x},$$

and

$$e_n = \frac{4\pi}{3} R_n^3 \rho_0. \quad (3)$$

$R_n$  is the radius of the cluster,  $v_x$  is the thermal exciton velocity, and  $\rho_0$  is the liquid density. The loss rate  $l_n$  is the sum of the evaporation rate  $e_n$  and the recombination rate  $n/\tau_n$ , where  $e_n$  is given by the Richardson-Dushman current

$$e_n = \gamma_x \left( \frac{m_x kT}{2\pi \hbar^2} \right)^{3/2} \frac{g_{n-1}}{f_1} \exp[-\phi + c\sigma n^{-1/3}], \quad (4)$$

$\gamma_x$  is the degeneracy of the exciton level, and  $\phi$  is the binding energy of the liquid with respect to the exciton. The quantity  $\sigma n^{-1/3} = (\frac{2}{3})4\pi R_n^2 \sigma n$  is the correction of  $\phi$  due to the surface energy per particle in the cluster, and  $\sigma$  is the surface tension. For very small clusters there are size-effect corrections which take the shell structure of the small complexes into account. The density-

functional theory has been used to investigate these size effects for small clusters with more than 20  $e-h$  pairs.<sup>9</sup> Corresponding calculations for still smaller clusters are not yet available. We disregarded these size effects in the present treatment. The temperature of the electronic excitations, which appears in the gain and evaporation rate, is usually different from the lattice temperature. Hildebrand *et al.*<sup>8</sup> measured for GaAs how the temperature of the electronic excitation increases with increasing frequency of the exciting laser light. Finally we note that the exciton-polariton effects which are also not considered in this model do not change the kinetics essentially, because the average thermal exciton wave number is typically much larger than the wave number belonging to the bottleneck region of the polariton spectrum.

The change of the exciton concentration needs special consideration. Its equation is

$$\frac{\partial f_1}{\partial t} = G(t) - \frac{f_1}{\tau_1} - 2g_1 f_1 + 2e_2 f_2 + \frac{2}{\tau_2} f_2 - \sum_{n=3}^{\infty} (g_{n-1} f_{n-1} - e_n f_n) \quad (5a)$$

$$= G(t) - \sum_{n=1}^{\infty} \frac{nf_n}{\tau_n} - 2j_1 - \sum_{n=2}^{\infty} j_n. \quad (5b)$$

The first two terms in Eq. (5a) describe the generation rate and the recombination rate of excitons, respectively. The third term describes the rate for the fusion of two excitons. A factor 2 appears in this term, because two excitons are lost if a molecule is formed by exciton fusion. The rate  $2e_2 f_2$  describes the reverse process, i.e., the molecule fission into two excitons. The fifth term of Eq. (5a) is the rate at which excitons are produced in the radiative decay of a molecule. The sum finally describes the net loss rate of excitons in the generation and evaporation processes of all clusters larger than the molecule. All of these terms have been grouped together conveniently in Eq. (5b).

From Eqs. (1)–(5b) one obtains the conservation law for the total number of  $e-h$  pairs. By defining

$$n_1 = \sum_{n=1}^{\infty} nf_n, \\ \dot{n}_1 = G(t) - \sum_{n=1}^{\infty} \frac{nf_n}{\tau_n} - 2j_1 - \sum_{n=2}^{\infty} j_n + \sum_{n=2}^{\infty} n(j_{n-1} - j_n),$$

we have

$$\dot{n}_1 = G(t) - \sum_{n=1}^{\infty} \frac{nf_n}{\tau_n} \quad (6)$$

because the currents add up to zero, i.e.,

$$2j_1 - \sum_{n=2}^{\infty} [nj_{n-1} - (n+1)j_n] \\ = - \sum_{n=2}^{\infty} nj_{n-1} + \sum_{n=1}^{\infty} (n+1)j_n = 0.$$

We solve numerically Eqs. (1)–(5) for the example of GaAs for various time dependences of the laser generation rate  $G(t)$  for  $1 \leq n \leq 150$ . For this purpose we use the simulation language CSMP,<sup>10</sup> which allows for the numerical integration of a large system of coupled ordinary differential equations. The material parameters for GaAs at  $T=6$  K are<sup>11</sup>  $m_x = 0.06 m_0$ ,  $\sigma = 7.6 \times 10^{-5}$  erg/cm<sup>2</sup>,  $\rho_0 = 5 \times 10^{16}$  cm<sup>-3</sup>,  $\tau_n = \tau = 1 \times 10^{-9}$  s,  $\phi = 6.4 \times 10^{-15}$  erg. The values of the plasma density and the binding energy have been deduced from a line-shape analysis of the observed gain spectrum,<sup>2,12</sup> because the theoretical calculations of these quantities for GaAs are not yet sufficiently accurate. The surface energy which has not been measured up to now is taken from a theoretical estimate by Rice.<sup>13</sup>

## II. CONTINUOUS EXCITATION

In order to study the intrinsic dynamics of the plasma instability, we assume a continuous laser generation rate which is switched on exponentially within a risetime  $t_r$ , i.e.,

$$G(t) = G_0 [1 - \exp(-t/t_r)]. \quad (7)$$

After a transient period the system will reach a steady state, in which all currents vanish (detailed balance),

$$j_n^s = 0, \\ G_0 = \sum_{n=1}^{\infty} \frac{nf_n}{\tau_n}, \quad (8)$$

as can be seen from Eqs. (1) and (5b). In Fig. 1 we show a series of cluster concentrations  $f_n(t)$  and cluster currents  $j_n(t)$  for various generation rates  $G_0$  and for a risetime  $t_r = 1$  ns. In Figs. 1(a) and 1(b) the value of  $G_0 = 4 \times 10^{24}$  cm<sup>-3</sup> s<sup>-1</sup> is still too low to produce a larger concentration of clusters with  $n > 1$ . The stationary exciton concentration is  $f_1^s = 1.43 \times 10^{14}$  cm<sup>-3</sup>.  $f_n^s$  is a monotonically decreasing function of  $n$ . The largest currents flow after a few nanoseconds. The threshold of the instability is reached at  $G_0 = 2.5 \times 10^{25}$  cm<sup>-3</sup> s<sup>-1</sup>, where  $f_n^s$  starts to have a relative maximum at  $n=6$  besides the absolute maximum at  $n=1$ . In Figs. 1(c) and 1(d) we show the development of  $f_n$  and  $j_n$  for a generation rate  $G_0 = 4 \times 10^{25}$  cm<sup>-3</sup> s<sup>-1</sup>, which is already above the threshold. One sees at around 10 ns a flooding of the larger cluster sizes, followed by a slow

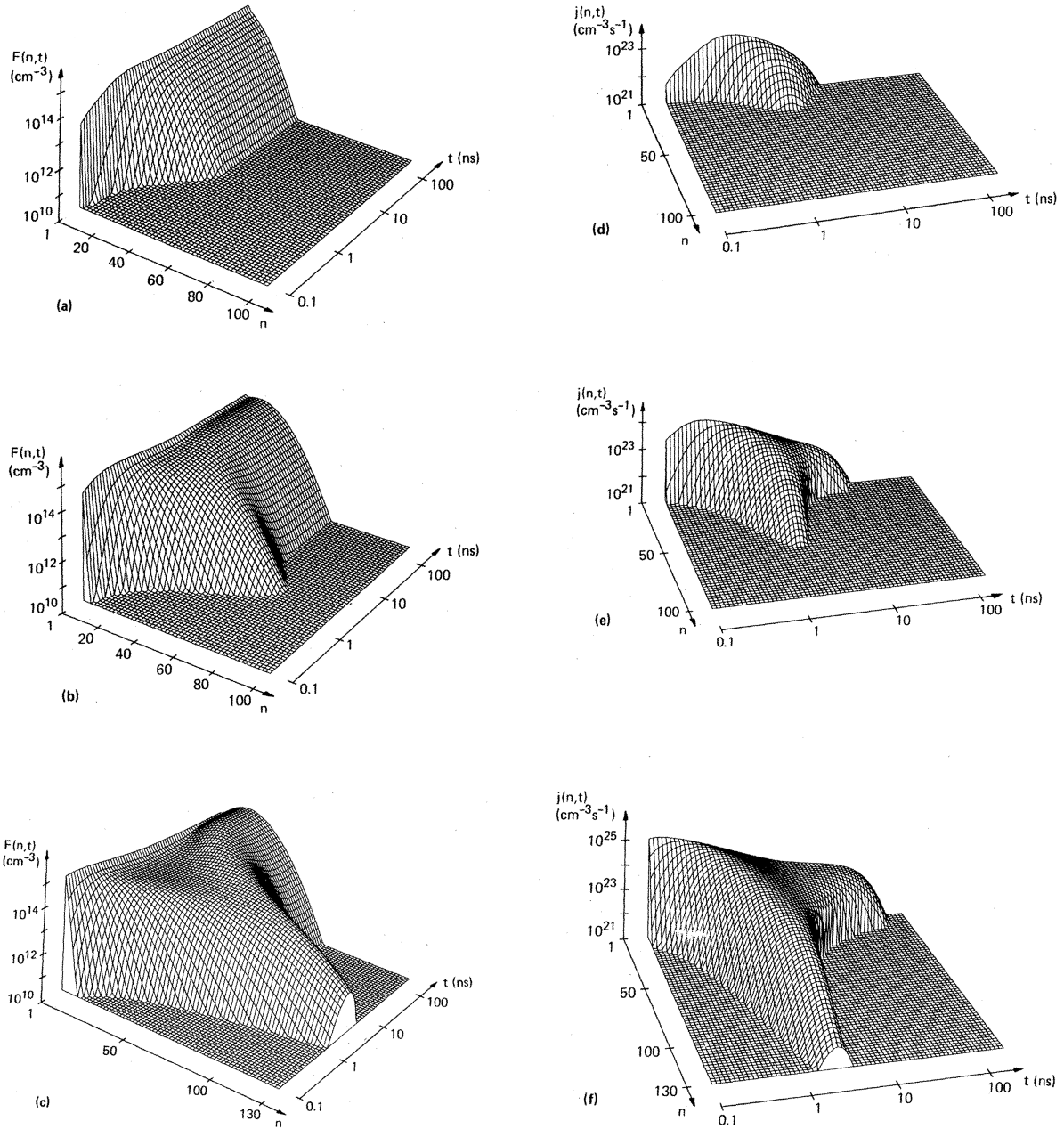


FIG. 1. Cluster concentrations (a), (b), and (c) and currents (b), (d), and (f) versus time and number of  $e$ - $h$  pairs per cluster for GaAs at  $T = 6$  K for three generation rates  $G_0 = 4 \times 10^{24} \text{ cm}^{-3} \text{ s}^{-1}$  (a) and (b),  $G_0 = 4 \times 10^{25} \text{ cm}^{-3} \text{ s}^{-1}$  (c) and (d), and  $G_0 = 4 \times 10^{26} \text{ cm}^{-3} \text{ s}^{-1}$  (e) and (f).

draining back into the steady-state distribution  $f_n^s$ . During this later stage the currents become negative, which is not shown on the logarithmic plots of  $j_n(t)$ . The stationary exciton concentration is  $f_1^s = 1.73 \times 10^{14} \text{ cm}^{-3}$ , with a second relative maximum occurring now at  $n = 9$  with  $f_9^s = 1.70 \times 10^{14} \text{ cm}^{-3}$ . We see that indeed only small clusters are formed. Finally, in Figs. 1(e) and 1(f),  $f_n(t)$  and  $j_n(t)$  are shown for a generation rate  $G_0$

$= 4 \times 10^{26} \text{ cm}^{-3} \text{ s}^{-1}$ , which is well above the plasma instability threshold. The flooding into larger clusters in the transient regime and the successive slow draining are here even more pronounced. The steady-state distribution is reached only after 100 ns. Although  $f_1^s$  is still a relative maximum with  $f_1^s = 1.93 \times 10^{14} \text{ cm}^{-3}$ , the absolute maximum is now at  $n = 19$  with  $f_{19}^s = 7.98 \times 10^{14} \text{ cm}^{-3}$ . The sequence of these distributions shows the intrinsic

characteristics of this nonequilibrium phase transition, such as the smallness of the formed cluster, the slow relaxation towards the steady-state distribution, and its weak first-order character.<sup>11</sup> In actual experiments, one uses pulses which are shorter than 100 ns in order to avoid heating. Therefore, we will study the kinetics of the  $e$ - $h$  cluster formation for nanosecond- and picosecond-pulse excitations.

### III. NANOSECOND-PULSE EXCITATION

Several experiments<sup>8</sup> have been reported in which an  $e$ - $h$  plasma has been generated by nanosecond-pulse excitation. Therefore, we studied the cluster formation and decay for nanosecond-pulse excitation, which we describe for convenience as a sine-square pulse:

$$G(t) = \begin{cases} G_0 \sin^2(\pi t/t_r), & t \leq t_r, \\ 0, & t > t_r. \end{cases} \quad (9)$$

We chose  $t_r = 14$  ns, which corresponds to a half-width of 7 ns.

In Figs. 2–4 we show a sequence of distributions for the following peak pump rates:  $G_0 = 5 \times 10^{24}$ ,  $2 \times 10^{25}$ , and  $5 \times 10^{25} \text{ cm}^{-3} \text{ s}^{-1}$ . For the lowest pump rate (Fig. 2) the excitons have the highest concentration of all clusters for all times, i.e.,  $f_1(t) > f_{n>1}(t)$ . For the two higher pump rates (Figs. 3 and 4) the exciton concentration is at the end of the pulse ( $t \approx t_r$ ) smaller than the concentrations of clusters with  $n \approx 10$  or 20 pairs, respectively. This can be seen more quantitatively from Figs. 5–7 in which we plotted the concentrations of a few selected clusters against time for the three generation rates. The curves show that at a later stage of the decay the molecule population is especially dominant until finally only the excitons

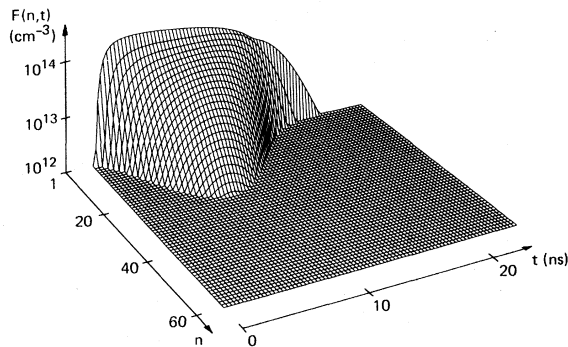


FIG. 2. Cluster concentrations versus time and number of  $e$ - $h$  pairs per cluster for GaAs at  $T = 6$  K under ns-pulse excitation;  $t_r = 14$  ns,  $G_0 = 5 \times 10^{24} \text{ cm}^{-3} \text{ s}^{-1}$ .

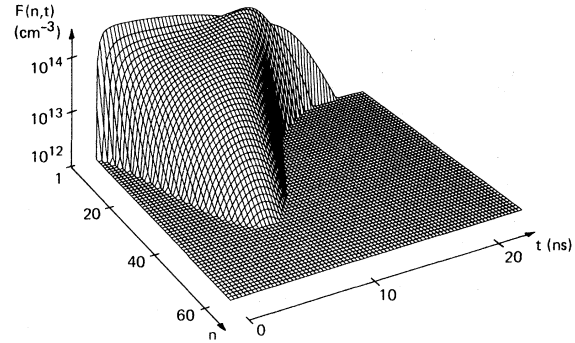


FIG. 3. As in Fig. 2 with  $G_0 = 2 \times 10^{25} \text{ cm}^{-3} \text{ s}^{-1}$ .

survive.

Up to now there exists no direct experimental observation of the cluster formation in direct-gap semiconductors. In order to stimulate experiments which are aimed at the observation of  $e$ - $h$  clusters, we calculate some quantities which are relevant for such experiments. They are as follows.

The total concentration of clusters of all sizes:

$$n_0 = \sum_{n=1}^{\infty} f_n, \quad (10)$$

The total concentration of all  $e$ - $h$  pairs:

$$n_1 = \sum_{n=1}^{\infty} n f_n. \quad (11)$$

The average number of pairs per cluster:

$$\langle n \rangle = n_1/n_0. \quad (12)$$

The shift of the chemical potential due to the finite cluster size:

$$\Delta \mu = \sum_{n=1}^{\infty} c \sigma n^{-1/3} \frac{f_n}{n_0}. \quad (13)$$

The maximum optical gain of the  $e$ - $h$  plasma is related to the total concentration of all  $e$ - $h$  pairs

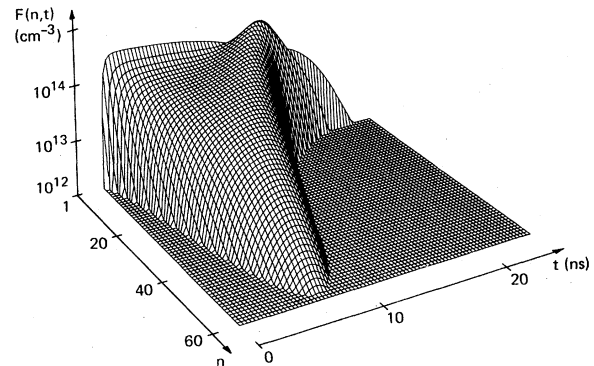


FIG. 4. As in Fig. 2 with  $G_0 = 5 \times 10^{25} \text{ cm}^{-3} \text{ s}^{-1}$ .

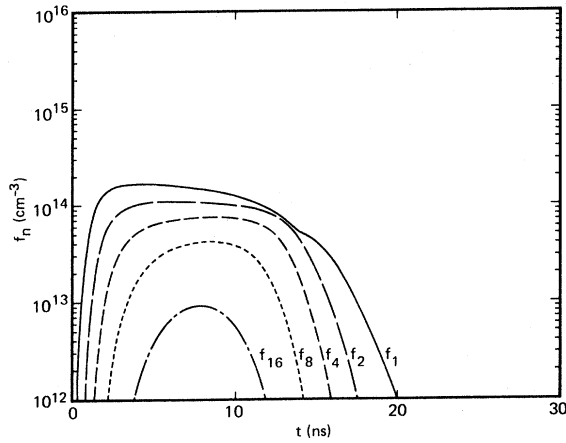


FIG. 5. Concentration of selected clusters versus time for GaAs at  $T=6$  K under ns-pulse excitation;  $t_p=14$  ns,  $G_0=5 \times 10^{24}$  cm $^{-3}$  s $^{-1}$ .

excluding the excitons:

$$g(\omega_{\max}) \propto (n_1 - f_1) \approx n_1. \quad (14)$$

The average number of pairs per cluster  $\langle n \rangle$  is too small to be detected by light scattering directly as in Ge.<sup>14</sup> More promising would be an attempt to deduce  $\langle n \rangle$  from the spikes in the photoconductivity of a  $p$ - $n$  junction when clusters are created in its neighborhood.<sup>15</sup> Finally, one can show that the optical gain spectrum  $g(\omega)$  changes from gain to absorption at  $\hbar\omega = \mu$ .<sup>16,17</sup> If  $e$ - $h$  clusters exist in the crystal, one has to average the contributions  $g_n(\omega)$  of all clusters

$$\langle g(\omega) \rangle = \sum_{n=1}^{\infty} g_n(\omega) \frac{f_n}{n_0}. \quad (15)$$

Close to  $\hbar\omega = \mu_n$  one can expand  $g_n(\omega)$  linearly, i.e.,  $g_n(\omega) \propto \hbar\omega - \mu_n$ , with  $\mu_n = dE_n/dn$ , where  $E_n$  is the ground-state energy  $E_n = E_\infty + 4\pi R_n^2 \sigma$ . Thus,

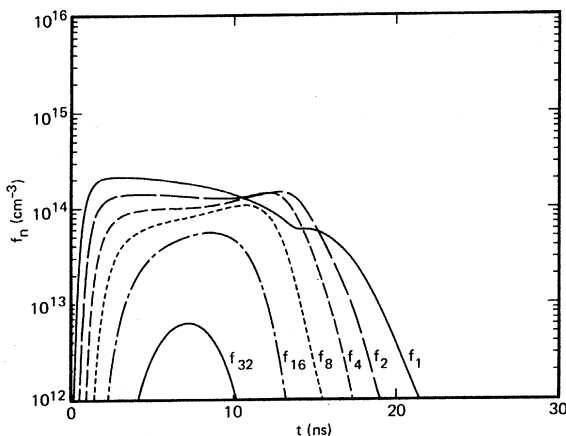


FIG. 6. As in Fig. 5 with  $G_0=2 \times 10^{25}$  cm $^{-3}$  s $^{-1}$ .

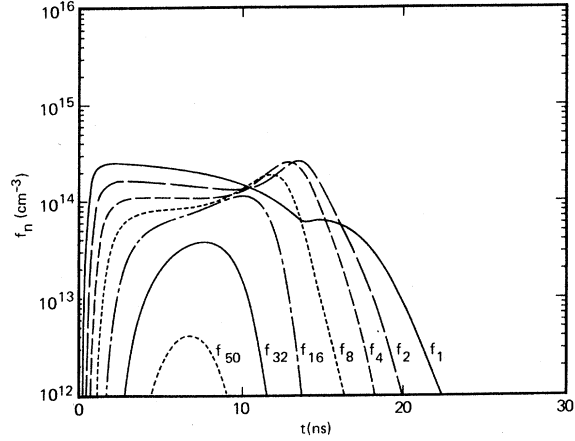


FIG. 7. As in Fig. 5 with  $G_0=5 \times 10^{25}$  cm $^{-3}$  s $^{-1}$ .

$\mu_n = \mu_\infty + c\sigma n^{-1/3}$ , where  $c$  is defined in connection with Eq. (4). Inserting this expansion in Eq. (15) gives

$$\langle g(\omega) \rangle \propto \hbar\omega - \mu_\infty - \Delta\mu, \quad (16)$$

where  $\Delta\mu$  is given by Eq. (13).

A time-resolved measurement of the shift of the zero crossing of the gain spectrum would therefore give a direct observation of the cluster size. Figures 8–10 show the time development of  $n_0$ ,  $n_1$ ,  $\langle n \rangle$ , and  $\Delta\mu$  for the above-mentioned peak-generation rates  $G_0$ . The total concentration of  $e$ - $h$  pairs  $n_1$  has to be smaller than the density  $\rho_0$  of the plasma liquid. At  $n_1 = \rho_0$  the crystal is homogeneously filled with liquid. Naturally, close to this limit the nucleation model is no longer accurate because of the cluster-cluster interactions which are not taken into account. Figure 10 shows that

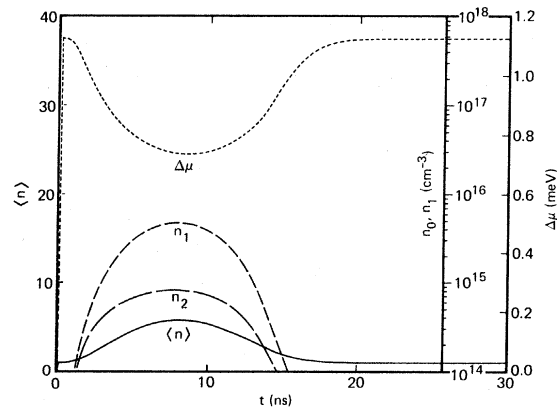


FIG. 8. Concentration of all clusters  $n_0$ , concentration of all  $e$ - $h$  pairs  $n_1$ , average number of  $e$ - $h$  pairs per cluster  $\langle n \rangle$ , and shift of the chemical potential  $\Delta\mu$  for GaAs at  $T=6$  K under ns-pulse excitation  $t_p=14$  ns,  $G_0=5 \times 10^{24}$  cm $^{-3}$  s $^{-1}$ .

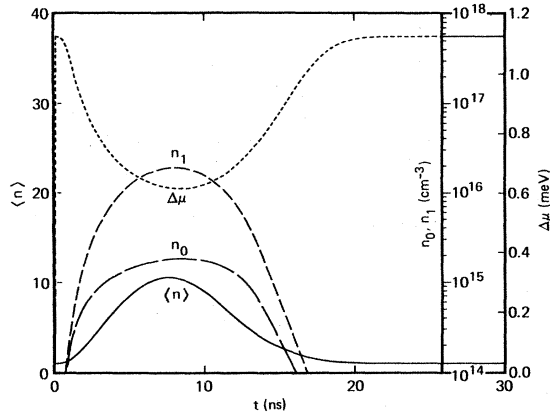


FIG. 9. As in Fig. 8 with  $G_0 = 2 \times 10^{25} \text{ cm}^{-3} \text{ s}^{-1}$ .

for a pump rate of  $G_0 = 5 \times 10^{25} \text{ cm}^{-3} \text{ s}^{-1}$  one generates at the peak of the pulse a homogeneous plasma liquid. With nanosecond-pulse excitation there exists no clear boundary of the coexistence region on the low-density side. Our results show that the coexistence region (i.e., the region where we have a considerable concentration of cluster with  $n > 1$ ) extends for nanosecond pulses roughly from  $1 \times 10^{25} \text{ cm}^{-3} \text{ s}^{-1} \lesssim G_0 \lesssim 5 \times 10^{25} \text{ cm}^{-3} \text{ s}^{-1}$ . The shift of the chemical potential are of the order of 0.5 meV at the peak of the pulses, where they could be most likely observed. The average number of pairs per cluster never gets larger than about 16, in striking contrast to Ge, where one finds typically  $\langle n \rangle \approx 10^6$ .

#### IV. PICOSECOND EXCITATION

In order to find the intrinsic relaxation times of a system of dense electronic excitations, direct-gap semiconductors have been excited by picosecond pulses.<sup>18</sup> In order to predict the dynamics of the cluster formation and decay under

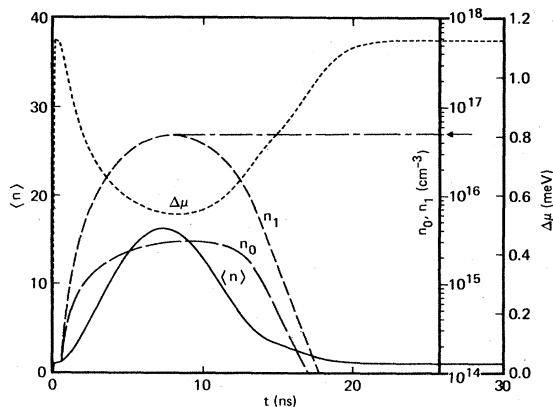


FIG. 10. As in Fig. 8 with  $G_0 = 5 \times 10^{25} \text{ cm}^{-3} \text{ s}^{-1}$ .

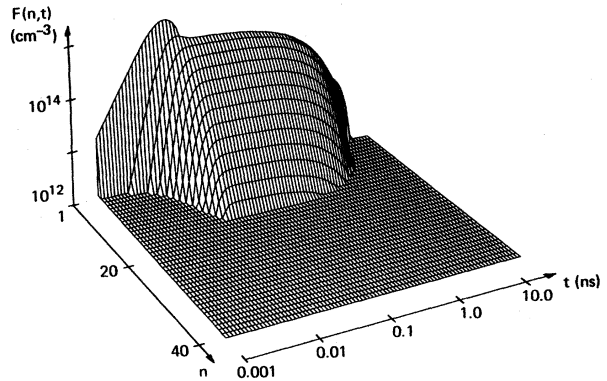


FIG. 11. Cluster concentration versus time and number of  $e-h$  pairs per cluster for GaAs at  $T = 6 \text{ K}$  under ps-pulse excitation;  $t_r = 20 \text{ ps}$ ,  $G_0 = 3 \times 10^{27} \text{ cm}^{-3} \text{ s}^{-1}$ .

picosecond excitation, we choose again a sine-square pulse [Eq. (9)] with  $t_r = 20 \text{ ps}$ , i.e., with a half-width of 10 ps. Figure 11 shows the development of the cluster distribution for a picosecond pulse with a peak-generation rate of  $G_0 = 3 \times 10^{27} \text{ cm}^{-3} \text{ s}^{-1}$ . The excitons are first considerably supersaturated, then the exciton concentration collapses, but only very small clusters are formed. After about 10 ns all cluster concentrations have decreased below  $10^{12} \text{ cm}^{-3}$ . The process of supersaturation and successive collapse of the exciton concentration can be seen quantitatively in Fig. 12. Figure 13 shows that the average number of pairs per cluster is  $\langle n \rangle \approx 3$  after the pulse. This is not due to an insufficient peak-generation rate, because at the peak of the pulse the concentration of all  $e-h$  pairs  $n_1$  is already close to the liquid density  $\rho_0$ . Owing to the

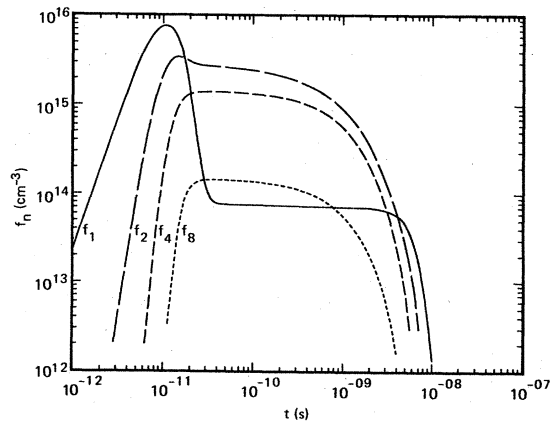


FIG. 12. Concentration of selected clusters versus time for GaAs at  $T = 6 \text{ K}$  under ps-pulse excitation;  $t_r = 20 \text{ ps}$ ,  $G_0 = 3 \times 10^{27} \text{ cm}^{-3} \text{ s}^{-1}$ .

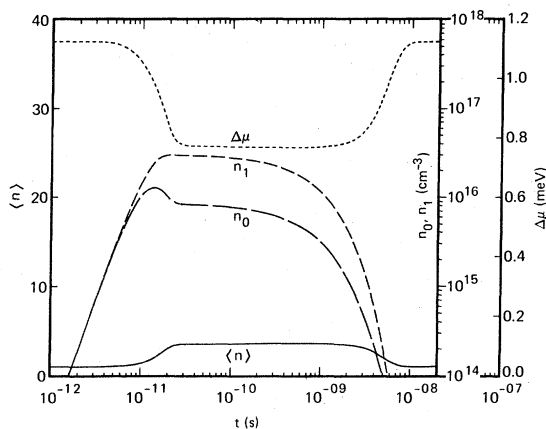


FIG. 13. Concentration of all clusters  $n_0$ , concentration of all  $e-h$  pairs  $n$ , average number of  $e-h$  pairs per cluster  $\langle n \rangle$ , and shift of the chemical potential  $\Delta\mu$  for GaAs at  $T = 6$  K under ps-pulse excitation;  $t_r = 20$  ps,  $G_0 = 3 \times 10^{27} \text{ cm}^{-3} \text{ s}^{-1}$ .

smallness of the complexes, the shift of the chemical potential is relatively large,  $\Delta\mu \approx 0.8$  meV. For a generation rate  $G_0 = 1 \times 10^{27} \text{ cm}^{-3} \text{ s}^{-1}$ , the average number of pairs per cluster is at most around 2. In conclusion, one can state that in

picosecond experiments one generates only minute clusters before one reaches generation rates which produce a homogeneous (at higher pump rates probably a compressed) plasma liquid.

How well the nucleation theory describes the onset of the plasma instability in direct-gap semiconductors can only be decided when experimental observations become available. The theory can be extended by taking into account the thermal mobility of clusters with  $n > 1$  and their fusion processes. The interaction of  $e-h$  pairs with the light field is much stronger for direct-gap semiconductors as, e.g., for Ge or Si. However, as long as the cluster concentration is not too high, a large optical gain cannot build up due to the smallness of the clusters.

#### ACKNOWLEDGMENTS

One of us (H.H.) acknowledges the hospitality of the IBM Research Laboratory in San Jose and the financial support of IBM Deutschland during a sabbatical leave from the University Frankfurt. This work is in part a project of the Sonderforschungsbereich Frankfurt/Darmstadt.

\*Permanent address: Institut für Theoretische Physik, Universität Frankfurt, Federal Republic of Germany.

<sup>1</sup>For reviews see Ya. Prokrovskii, *Phys. Status Solidi A* **11**, 385 (1972); C. D. Jeffries, *Science* **189**, 955 (1975); J. C. Hensel, T. G. Phillips, and G. A. Thomas, in *Solid State Physics*, edited by H. Ehrenreich, F. Seitz, and D. Turnbull (Academic, New York, 1977), Vol. 32, p. 1.

<sup>2</sup>R. N. Silver, *Phys. Rev. B* **11**, 1569 (1975); **12**, 5689 (1975); **16**, 797 (1976).

<sup>3</sup>R. M. Westervelt, *Phys. Status Solidi B* **74**, 727 (1976).

<sup>4</sup>J. L. Staehli, *Phys. Status Solidi B* **75**, 451 (1976).

<sup>5</sup>S. W. Koch and H. Haug, *Phys. Status Solidi B* **95**, 155 (1979).

<sup>6</sup>F. F. Abraham, *Homogeneous Nucleation Theory* (Academic, New York, 1974).

<sup>7</sup>H. Haug and S. W. Koch, in *Dynamics of Synergetics*, edited by H. Haken (Springer, Berlin, 1980).

<sup>8</sup>See, e.g., R. F. Leheny and J. Shah, *Phys. Rev. Lett.* **37**, 871 (1976); O. Hildebrand, E. Göbel, K. M. Romanek, H. Weber, and G. Mahler, *Phys. Rev. B* **17**, 4775 (1978); G. O. Müller and R. Zimmerman, in *Proceedings of the Fourteenth International Conference on the Physics of Semiconductors, Edinburgh, 1978*, edited by B. L. H. Wilson (The Institute of Physics, Bristol, 1978), p. 165; K. Bohnert, G. Schmieder, and C. Klingshirn, *Phys. Status Solidi B* **98**, 175 (1980).

<sup>9</sup>J. H. Rose, R. Pfeiffer, L. M. Sander, and H. B. Shore, *Solid State Commun.* **30**, 697 (1979).

<sup>10</sup>Continuous System Modeling Program III (CSMPIII), Program Reference Manual SH19-7001-2, Program Number 5734-XS9, IBM Corporation, Data Processing Division, White Plains, New York (1975).

<sup>11</sup>S. W. Koch and H. Haug, *Phys. Lett.* **75A**, 250 (1979). Note the misprints of the values of  $\sigma$  in Table I.

<sup>12</sup>H. Haug and D. B. Tran Thoai, *Phys. Status Solidi B* **98**, 581 (1980); S. Schmitt-Rink, D. B. Tran Thoai, and H. Haug, *Z. Phys. B* **39**, 25 (1980); *Solid State Commun.* **36**, 381 (1980).

<sup>13</sup>T. M. Rice, *Phys. Rev. B* **9**, 1540 (1974).

<sup>14</sup>Ya. Prokrovskii and K. I. Svistanova, *Zh. Eksp. Teor. Fiz. Pis'ma Red* **13**, 297 (1971) [*JETP Lett.* **13**, 212 (1971)].

<sup>15</sup>See, e.g., V. M. Asnin, A. A. Rogachen, and N. I. Salin Sablin, *Zh. Eksp. Teor. Fiz. Pis'ma Red* **11**, 162 (1970) [*JETP Lett.* **11**, 99 (1970)]; C. Benoît à la Guillaume, M. Voos, F. Salvan, J. M. Laurant, and A. Bonnot, *C. R. Acad. Sci. Ser. B* **272**, 236 (1978).

<sup>17</sup>For a review of the optical properties of highly-excited direct-gap semiconductors, see C. Klingshirn and H. Haug, *Phys. Rep. C*, in press.

<sup>18</sup>See, e.g., D. Auston, in *Proceedings of the Fourteenth International Conference on the Physics of Semiconductors, Edinburgh, 1978*, edited by B. L. H. Wilson (The Institute of Physics, Bristol, 1978), p. 73; C. V. Shank, R. L. Fork, R. F. Leheny, and J. Shah, *ibid.*, p. 493; D. v. d. Linde and R. Lambrich, *Phys. Rev. Lett.* **42**, 1090 (1979).